21

Microneedle-Assisted Transdermal Delivery of Opioid Antagonists for the Treatment of Alcoholism

Stan L. Banks[1,2], Audra L. Stinchcomb[1,2,3] and Kalpana S. Paudel[1,4]
[1]*Department of Pharmaceutical Sciences, University of Kentucky College of Pharmacy, Lexington, Kentucky,*
[2]*AllTranz Inc., Lexington, Kentucky,*
[3]*Department of Pharmaceutical Sciences, University of Maryland School of Pharmacy, Baltimore, MD*
[4]*Department of Pharmaceutical Sciences, Midway College School of Pharmacy, Paintsville, KY*
USA

1. Introduction

It has been estimated that nearly 19 million Americans or 8% of the U.S. population need treatment for an alcohol problem. Alcohol dependence accounts for approximately 100,000 deaths each year. Alcoholism abuse and dependence costs the United States $185 billion dollars in direct and indirect social costs per year with more than 70% of the cost attributed to lost productivity.

Current treatments for alcohol dependence include acamprosate calcium, disulfiram, and naltrexone (NTX). NTX is a potent competitive opioid antagonist with high affinity for the mu-opioid receptor. NTX is currently available in an oral 50 mg tablet (ReVia® and generics) as well as a 380 mg depot injection for the treatment of opiate and alcohol addiction (Vivitrol®; PDR, 1996). The dosage forms have had limited success due to poor oral bioavailability (5-40%), intense side effects such as nausea and stomach pain, as well as inconsistent release from the depot form (Vivitrol®; PDR, 1996). An alternative approach to circumvent drawbacks from oral therapy and painful depot injections to treat alcoholism is transdermal delivery. By initially limiting the input of the drug dose directly to the systemic circulation, extensive metabolism in the liver is bypassed, thereby increasing efficacy and decreasing the chance of deleterious side effects. Transdermal drug delivery systems are trouble-free outpatient products, and monthly reoccurring healthcare visits to receive a painful injection can be avoided.

Opioid antagonists such as NTX, naloxone and nalmefene, a nonselective opioid antagonist, have been studied for delivery by the transdermal route for the treatment of alcohol dependence. However, most of the opioid antagonists do not have suitable physicochemical properties for required therapeutic skin permeation rates from passive-delivery. Previous attempts to deliver a controlled therapeutic dose of NTX through the skin have been unsuccessful in achieving desirable permeation rates in the high end of the therapeutic

range (Hammell et al., 2004; Pillai et al., 2004; Vaddi et al., 2005). NTX's primary metabolite, 6-β-naltrexol (NTXOL), is formed by reduction at the 6-keto group. NTXOL, which may provide a longer duration of action than NTX, also does not have optimal physicochemical properties for transdermal delivery (King et al., 1997; Verebey et al., 1976). NTXOL's maximum flux values have been reported to be 6-fold less than that of the parent NTX (Paudel et al., 2005). Approaches ranging from prodrug synthesis to codrug formation have been applied to enhance permeation of NTX and NTXOL through the skin with limited successes (Kiptoo et al., 2006; Valiveti et al., 2005).

The most recent approach to deliver therapeutically relevant levels of NTX is with the application of microneedle (MN) arrays to the skin (Wermeling et al., 2008). NTXOL has also been evaluated for MN skin permeation enhancement in hairless guinea pigs (GP) (Banks et al., 2010). Microneedles, composed from stainless steel, biodegradable polymers, and silicon, provide an aqueous conduit for drug to bypass the stratum corneum and enter the systemic circulation (Prausnitz, 2004; Prausnitz et al., 2005). MN study, while in its infancy, has focused on a broad range of compounds such as insulin, desmopressin, oligonucleotides, and vaccines for permeation enhancement (Cormier et al., 2004; Coulman et al., 2006; Gardeniers et al., 2003; Martanto et al., 2004; Mikszta et al., 2002; Prausnitz, 2004). MNs have been mostly used either as a pretreatment to permeabilize skin before applying a patch or with drug coated onto the MN array for rapid dissolution and release in the skin (Cormier et al., 2004; Martanto et al., 2004; Prausnitz, 2004).

Previous studies have shown that the transdermal flux of NTX and NTXOL can be enhanced by MN and can be optimized by using MN in combination with charged (protonated) drugs that have increased solubility in an aqueous patch reservoir and increased permeability through aqueous pathways created by MN in the skin (Banks et al., 2008). Another study determined the lifetime of MN-created aqueous pore pathways (Banks et al., 2010). MN pore lifetime was estimated by pharmacokinetic evaluation, transepidermal water loss (TEWL) and visualization of MN-treated skin pore diameters using light microscopy. A 3.6-fold enhancement in steady-state plasma concentration was observed *in vivo* with MN treated skin with the hydrochloride (HCl) salt of NTXOL as compared to NTXOL base. TEWL measurements and microscopic evaluation of stained MN-treated GP skin indicated the presence of pores, suggesting a feasible nonlipid bilayer pathway for enhanced transdermal delivery. Overall, MN-assisted transdermal delivery appeared viable for at least 48 h after MN-application.

It has been shown that formulation, specifically the viscosity of the formulation, influences the MN-enhanced transdermal transport of NTX·HCl (Milewski & Stinchcomb., 2011). Another study has combined microneedle skin pretreatment with the use of a highly water-soluble PEGylated NTX prodrug for further improvement in the percutaneous flux of NTX (Milewski et al., 2010). The main drawback of MN-assisted delivery, however, is that the micropores begin to close between 48-72 hour (Banks et al., 2010) and hence it is not possible to achieve sustained delivery of the drug for a prolonged period. A recent study has shown that by using diclofenac, a nonspecific COX inhibitor, daily with NTX enables the delivery of the drug over a 7 day period in hairless GP (Banks et al., 2011).

An *in vitro/in vivo* correlation (IVIVC) is an integral relationship in pharmaceutical dosage form development. Defined by the FDA, an IVIVC is a predictive model describing the relationship between an *in vitro* property of a dosage form and relevant *in vivo* response (FDA). In the case of transdermal delivery, the *in vitro* property is the rate of permeation or release through the skin while the *in vivo* response is the plasma drug concentration. An

IVIVC is an important aspect of transdermal delivery, because it gives validation to *in vitro* diffusion studies. Building confidence into the *in vitro* model is a cost and time saving factor that affords screening of multiple compounds and only testing the most successful *in vivo*. Previous studies looking at transdermal delivery of NTX prodrugs and a highly lipophilc drug, delta 8-THC, showed good correlation with the hairless GP pharmacokinetic model and *in vitro* flow through diffusion cell data (Valiveti et al., 2004a). The approach to deliver NTX at therapeutically relevant levels that has recently been studied is to use the water soluble form of NTX aided by MN facilitated permeation of the skin (Banks et al., 2008). In this present study, we describe IVIVC of NTX through MN treated skin. *In vitro* skin permeation studies were carried out across MN treated GP and human skin with a gel comprised of the hydrophilic HCl salt form of NTX. Then, *in vivo* studies were carried out in GP utilizing a MN gel patch delivery system to establish an IVIVC in GPs. Finally, the *in vitro* human skin data was compared with data from a previous healthy human volunteer study (Wermeling et al., 2008) to establish the human IVIVC.

2. Materials and methods

2.1 Materials

NTX·HCl was purchased from Mallinckrodt Inc. (St. Louis, MO, USA). Hanks' balanced salts modified powder and propylene glycol was purchased from Sigma Aldrich (St. Louis, MO, USA). Ammonium citrate was purchased from Alfa Aesar (Ward Hill, MA, USA). Sodium bicarbonate, 4-(2-hydroxyethyl)-1-piperazineethanesulfonic acid (HEPES), gentamicin sulfate, ammonium acetate, ethyl acetate, acetonitrile (ACN), triethylamine (TEA) and trifluoroacetic acid (TFA) were obtained from Fisher Scientific (Fairlawn, NJ, USA). A Barnstead nanopure Diamond Ultrapure water system was used for all aqueous solutions (Barnstead International, Dubuque, IA, USA). 1-Octanesulfonate was purchased from Regis Technologies, Inc (Morton Grove, IL, USA). Natrosol® (Hydroxyethylcellulose250HHX PHARM) was a gift from Hercules, Inc. (Wilmington, DE, USA). Benzyl Alcohol was purchased from Spectrum Chemical MFG. Corp. (Gardena, CA, USA).

2.2 Microneedle fabrication

In-plane microneedle rows with five microneedles were cut from stainless steel sheets (Trinity Brand Industries, SS 304, 75 mm thick; McMaster-Carr, Atlanta, GA, USA) using an infrared laser (Resonetics Maestro, Nashua, NH, USA) using methods previously described (Martanto et al., 2004) in the laboratory of Dr. Mark Prausnitz at the Georgia Institute of Technology. Briefly, the microneedle row was first drafted in AutoCAD software (Autodesk, Cupertino, CA, USA). Using this design, the infrared laser cut microneedles into the stainless steel sheet. The microneedle rows were then cleaned with detergent (Alconox, White Plains, NY, USA) to de-grease the surface and remove part of the slag and oxides deposited during laser-cutting. To completely clean the slag and debris and to sharpen microneedle tips, microneedle rows were electropolished in a solution containing glycerin, ortho-phosphoric acid (85%) and water in a ratio of 6:3:1 by volume (all chemicals, Fisher Scientific, Fair Lawn, NJ, USA). Electropolishing was performed in a 300 ml glass beaker at 70°C, a stirring rate of 150 rpm, with a current density of 1.8 mA/mm^2 applied for 15 min. A copper plate was used as the cathode (negative), while microneedles acted as the anode (positive). The electropolished microneedle rows were then cleaned by alternatively dipping in 25 % nitric acid (Fisher Scientific) and deionized water with a total of three repetitions. A

final rinse was performed under running deionized water before drying under pressurized air. Dry microneedle rows were stored in air-tight containers until later use. MN arrays for human studies were fabricated to produce patches containing 50MNs arranged in 5x10 arrays of MNs. Each MN measured 620 µm in length, 160 µm in width at the base, and 1 µm in radius of curvature at the tip. For *in vitro* studies and *in vivo* GP studies, each MN measured 750 µm in length, had a base width of 180 µm, and <1 µm radius in curvature at the tip. The distance between individual MNs was approximately 1 mm.

2.3 16% NTX·HCl gel formulation

The NTX gel formulation used for *in vitro* and *in vivo* studies consisted of NTX·HCl, (16.0%), propylene glycol (60.75%), sterile water for injection (20.25%), benzyl alcohol (1.0%) and hydroxyethylcellulose (2.0%). For human studies, the same formulation composition was used except that the gel was formulated, prepared, and tested according to current good manufacturing practices as outlined by the FDA and was carried out in collaboration with Coldstream Laboratories, Inc., formerly named The Center for Pharmaceutical Science and Technology (Wermeling et al., 2008).

2.4 *In vitro* studies

2.4.1 *In vitro* diffusion studies across full thickness hairless GP and human skin

Full thickness hairless GP skin was harvested from euthanatized animals. Animal studies were approved by the University of Kentucky IACUC. Human skin harvested during abdominoplasty was used for the diffusion studies. Human tissue use was approved by the University of Kentucky Institutional Review Board. Skin sections were obtained by removing the subcutaneous fatty tissue by scalpel dissection, and were stored at -20°C. A PermeGear flow-through (In-Line, Riegelsville, PA, USA) diffusion cell system was used for the skin permeation studies. Skin used for microneedle treatment was placed on a wafer of polydimethylsiloxane polymer, which mimicked the underlying mechanical support of tissue because of its comparable structural flexibility and elasticity. The human skin was pierced 20 times with an array containing 5 MN (Figure 1) (i.e., to make a total of 100 individual and non-over lapping piercings) before mounting the skin in the diffusion cell. Diffusion studies to determine flux values for GP skin were performed in such a way that only 3 insertions were made to obtain 15 individual and non-overlapping MN insertions. The insertion of MN into skin was carried out manually by applying gentle finger pressure followed by instantaneous removal. MN's were distributed evenly within the 0.95 cm^2 area of skin and could easily be visualized after each 5 MN insertion, as to prevent reapplication in the same area. Single MN sections of 5 were used simply out of ease for the experimental procedure. If any damage to an MN section was observed the section was replaced. Cells containing MN treated skin showed no presence of receiver solution back flow into the donor compartment. Untreated skin samples were simply placed in the diffusion cells. Diffusion cells were kept at 32°C using a circulating water bath. Data were collected using skin from a single guinea pig or human.

donor with three cells for untreated formulations and 3-4 cells for the MN treated formulations. The physiological receiver solution was HEPES-buffered Hanks' balanced salts with gentamicin at pH 7.4, and the flow rate was adjusted to 1.1 ml/h. Each cell was charged with 0.25 ml of the gel spread over the skin in the donor compartment of the chamber. The diffusion cells were covered with a stopper to prevent evaporation. Samples

were collected from the receiver compartment in six-hour increments over 48 h. All samples were stored at 4°C until analyzed by HPLC.

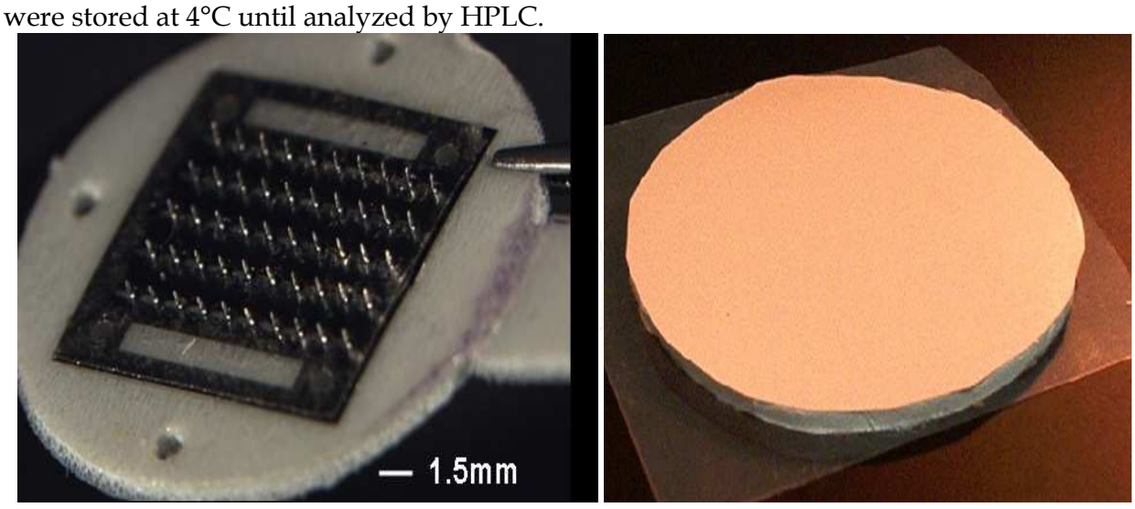

Fig. 1. Left depicts a 50 MN array used in human and GP studies and right shows a protective gel patch covering.

2.4.2 HPLC analysis

Quantitative analysis of NTX concentrations in receiver samples was carried out using a modification of the HPLC assay described by Hussain et al. (Hussain et al., 1987; Paudel et al., 2005). This HPLC analysis was performed as reported by Vaddi et al. (Vaddi et al., 2005). The receiver samples were diluted 10 fold with acetonitrile and injected directly into the HPLC. The HPLC system consisted of a Waters 717plus autosampler, a Waters 1525 Binary HPLC pump, and a Waters 2487 dual wavelength absorbance detector with Waters Breeze™ software (Milford, Massachusetts, USA). A Brownlee (Wellesley, Massachusetts, USA) C-18 reversed-phase Spheri-5 µm column (220 x 4.6 mm) with a C-18 reversed phase 7 µm guard column (15 x 3.2 mm) by Perkin Elmer® was used with the UV detector set at a wavelength of 215 nm. The mobile phase for NTX was 70:30 ACN: 0.1% TFA with 0.065% 1-octane sulfonic acid sodium salt, adjusted to pH 3.0 with TEA, and samples were run at a flow rate of 1.5 ml/min with a run time of 5 min.

2.4.3 *In vitro* data analysis

The cumulative quantity of drug collected in the receiver compartment was plotted as a function of time. The flux value for a given experiment was obtained from the slope of the steady state portion of the cumulative amount of drug permeated plotted over time. Apparent permeability coefficient values were calculated from Fick's First Law of diffusion:

$$\frac{1}{A}\left(\frac{dM}{dt}\right) = J_s = K_p \Delta C \tag{1}$$

where J_s is the flux at steady state (nmol/cm²/h), M is the cumulative amount of drug permeating through the skin, t is time, A is the area of the skin (0.95 cm²), K_p is the effective permeability coefficient in cm/h, and ΔC is the difference in concentrations of NTX in the donor and receiver components. Sink conditions were maintained in the receiver solution

for the duration of the experiment; thus ΔC was approximated by the initial drug concentration in the donor compartment.

2.5 *In vivo* hairless GP and human studies

2.5.1 Transdermal protective covering patches and dosing regimen

The transdermal covering was prepared as described by Wermeling et al. (Wermeling et al., 2008). Briefly, the transdermal occlusive protective covering patches of NTX·HCl (6.7 cm^2) were fabricated by sandwiching a rubber ringed barrier to create a reservoir between a drug-impermeable backing membrane (Scotchpak™ #1109 SPAK 1.34 MIL Heat Sealable Polyester Film, 3M Drug Delivery Systems, St. Paul, MN, USA) and an ARcare® 7396 adhesive around the edge of the nitrile spacer (Adhesive Research, Inc., Glen Rock, PA, USA). The impermeable backing laminate was adhered to the FDA approved medical grade nitrile retaining ringed barrier from Ilene Industries (Shelbyville, TN, USA) with ARcare® 7396. Finally, ARcare® 7396 was placed on the bottom of the rubber ringed barrier to maintain intimate contact with the skin and prevent evaporation of the 500 µL gel formulations. The protective patch was placed on a release liner composed of Scotchpak™ 9742 (3M Drug Delivery Systems, St. Paul, MN, USA). Human subjects were dosed with a total of 400 MN insertions and 2 g of gel. That is, the dose per patch was 0.5 mg gel and 100 MN insertions (Wermeling et al., 2008). MN arrays were applied manually to humans by only one clinician, after training to reproducibly apply with the same force. The same procedure was followed for the control subjects without the application of microneedle arrays. The gel patch systems were left in place on the skin for 72 hours, during which plasma samples were collected for LC-MS analysis of NTX and its active metabolite, NTXOL. The above described system was utilized on hairless GP (n=4) with only 15 MN insertions and 1 gel patch assembly system for 72 hours. For these studies, the insertion of MN was manual by applying gentle finger pressure followed by instantaneous removal. As in the human studies, only one researcher applied MN arrays to GP manually to reproducibly apply with the same force. The gel patch system was applied on the dorsal region of the hairless GP. Bio-occlusive tape was applied over the patches followed by a protective stocking. Samples were collected for LC-MS analysis. All plasma samples were stored at -70°C until analyzed.

2.5.2 Plasma sample extraction procedure

Samples were prepared and analyzed as described by a modified method as described by Paudel *et al*. (Paudel et al., 2005). One-hundred µL of plasma was extracted with 500 µL of ethyl acetate. The mixture was vortexed for 30 s and centrifuged at 10,000 x g for 20 min. The pellet and supernatant were placed in a -20°C freezer for 15 minutes to freeze the aqueous pellet. The supernatant was pipetted into a 3 ml glass test tube and evaporated under nitrogen at 37°C. The residue was reconstituted with 100 µL of ACN and sonicated for 15 min. The samples were transferred into autosampler vials containing low volume inserts, and 20 µL was injected onto the HPLC column.

2.5.3 Liquid chromatography

Chromatography was performed on a Waters Symmetry® C_{18} (2.1 x 150mm, 5 µm) column at 35°C with a mobile phase consisting of ammonium acetate (2 mM) containing 0.01 mM of ammonium citrate:ACN (65:35 v/v) at a flow-rate of 0.25 ml/min.

2.5.4 Mass spectrometry

The system consisted of HPLC with mass spectrometry detection (LC-MS) equipped with a Waters Alliance 2695 pump, Alliance 2695 autosampler, and a Micromass ZQ detector (Milford, MA) using electrospray ionization (ESI) for ion production. Selected ion monitoring (SIM) was performed in positive mode for NTX, m/z 324 $[M+H]^+$ and NTXOL, m/z 344 $[M+H]^+$. Capillary voltage was 4.5 kV and cone voltage was 30 V. The source block and desolvation temperatures were 120°C and 250°C, respectively. Nitrogen was used as a nebulization and drying gas at flow rates of 50 and 450 L/h, respectively.

2.5.5 *In vivo* data analysis

The pharmacokinetic analysis of NTX plasma concentration versus time profiles after MN treatment and gel patch application was carried out by fitting the data to a non-compartmental model with extravascular input (WinNonlin Professional, version 4.0, Pharsight Corporation, Mountain View, CA). The data generated were analyzed to determine peak concentration (C_{max}), steady state concentration (C_{ss}), lag time to steady state concentration (t_{lag}), and area under the plasma concentration time course from 0 to 72 h (AUC_{0-72}). The steady state plasma concentration of NTX after the application of patches was calculated by using the equation:

$$C_{ss} = AUC_{0-t}/\text{time} \tag{2}$$

2.5.6 *In vitro*/*In vivo* correlation

The predicted steady state plasma concentrations of NTX in the GP following the application of the TTS patch was calculated from the *in vitro* steady state flux by using the following equation:

$$C_{SS} = \frac{J_{SS}A}{CL} \tag{3}$$

where 'Css' is the predicted steady state plasma concentration (ng/ml); 'J_{ss}' is the steady state flux across human or GP skin; 'A' is area of the applied patch (26.8 or 6.7 cm^2 in humans or GP, respectively); 'CL' is the total body clearance in humans or GP.

Statistical analysis of the *in vivo* data obtained after the transdermal application of the patches was performed by one-way ANOVA using SigmaStat.

3. Results

3.1 16.0% NTX·HCl gel characterization

All of the release testing and stability testing of the 16.0% NTX·HCl gel was performed in Coldstream Laboratories, Inc. in accordance to cGMP regulations set forth by the FDA and the standard operating procedures of the facility. All curves generated for HPLC standard analysis of the gel had an average correlation value (r^2) of 0.999 ± 0.001 and precision for the assay had a % RSD of 0.67%. The solubility determined prior to formulation scale-up of NTX·HCl was 171.9 mg/ml. Thus, a 16% gel would be approximately 93.7% of the saturation limit, providing a satisfactory driving force according to Fick's first law of diffusion. The percent label claim of the gel at the product release testing, 1.5 months, and 5 months at 25°C/60% relative humidity was 97.0 ± 0.7%, 105.6 ± 3.5%, and 97.8 ± 1.7%,

respectively. All of the HPLC results were within the 90.0 – 110.0% of the specifications for label claim. The gel was clear, colorless and transparent, and over time a yellowish tint was observed. The pH was measured at 4.96 ± 0.03 and the viscosity was 16,859 ± 437 cP. Overall, the formulation was within percent label claim, had a pharmaceutically elegant appearance, excellent consistency to maintain intimate contact with the skin, and a skin compatible pH.

3.2 *In vitro* diffusion studies

3.2.1 HPLC validation

Calibration plots were prepared using NTX standards with the final concentrations over a range of 0.1-25 µg/ml. The correlation coefficient (r^2) obtained was 0.9997 for standard curves. The lower limit of quantification (LLOQ) was 0.1 µg/ml and the limit of detection (LOD) was 0.05 µg/ml.

3.2.2 *In vitro* diffusion studies across full thickness hairless GP skin

From cumulative permeation profiles the flux could be ascertained from the linear portion (apparent steady state). Extrapolation of this linear curve to the x-axis gives the lag-time to steady state. Figure 2 shows a cumulative NTX profile from 16% NTX·HCl gel on full thickness GP skin with 15 MN insertions and control intact GP skin that had no MN treatment. Table 1 shows the fluxes observed with 15 MN insertions as well as fluxes obtained from intact GP skin. Permeability coefficients and solubility are also reported. As observed in Table 1, a significant difference was observed ($p < 0.05$) in both flux and permeability parameters.

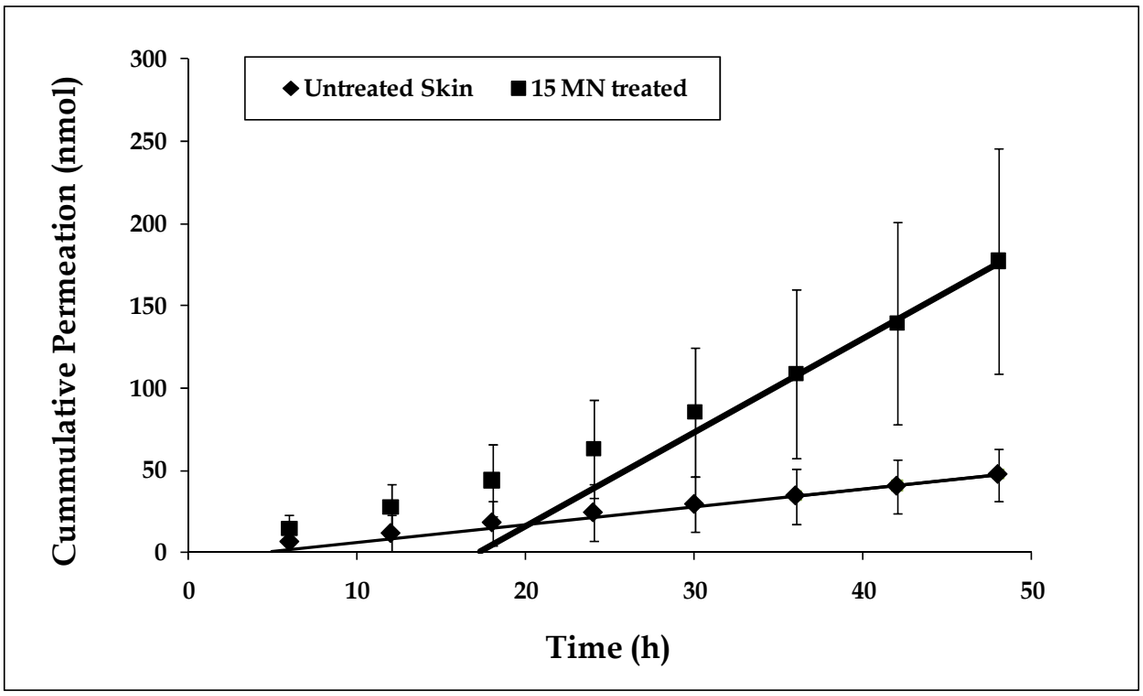

Fig. 2. Cumulative amount of NTX·HCl permeated through 15 MN treated and intact GP skin.

In vitro Study	MN treatment	Flux (nmol/cm²/h)	Kp (x 10⁵cm/h)
GP Skin	No MN	1.1 ± 0.9	0.26
	† MN treated	6.0 ± 1.5	1.4
Human Skin	No MN	0.13 ± 0.01	0.03
	†† MN treated	39.0 ± 13.1	9.2

† GP skin treated with 15 MN insertions for *in vitro* study.
†† Human skin treated with a total of 100 MN insertions for *in vitro* study

Table 1. *In vitro* permeation of a 16.0% NTX·HCl gel through human and GP skin

3.2.3 *In vitro* diffusion studies across full thickness human skin

Flux values and permeation profiles of NTX in human skin can be observed in table 1 and figure 3, respectively. Again, as shown in GP skin, a significant increase in flux ($p < 0.05$) was observed when comparing MN treated skin (39.0 ± 13.1 nmol/cm²/h) to intact full thickness skin (0.13 ± 0.01 nmol/cm²/h). Flux and permeability coefficients from MN treated skin were enhanced 300-fold when compared to intact full thickness human skin. As seen in figure 3, there is also a reduction in lag time when the skin is exposed to MN.

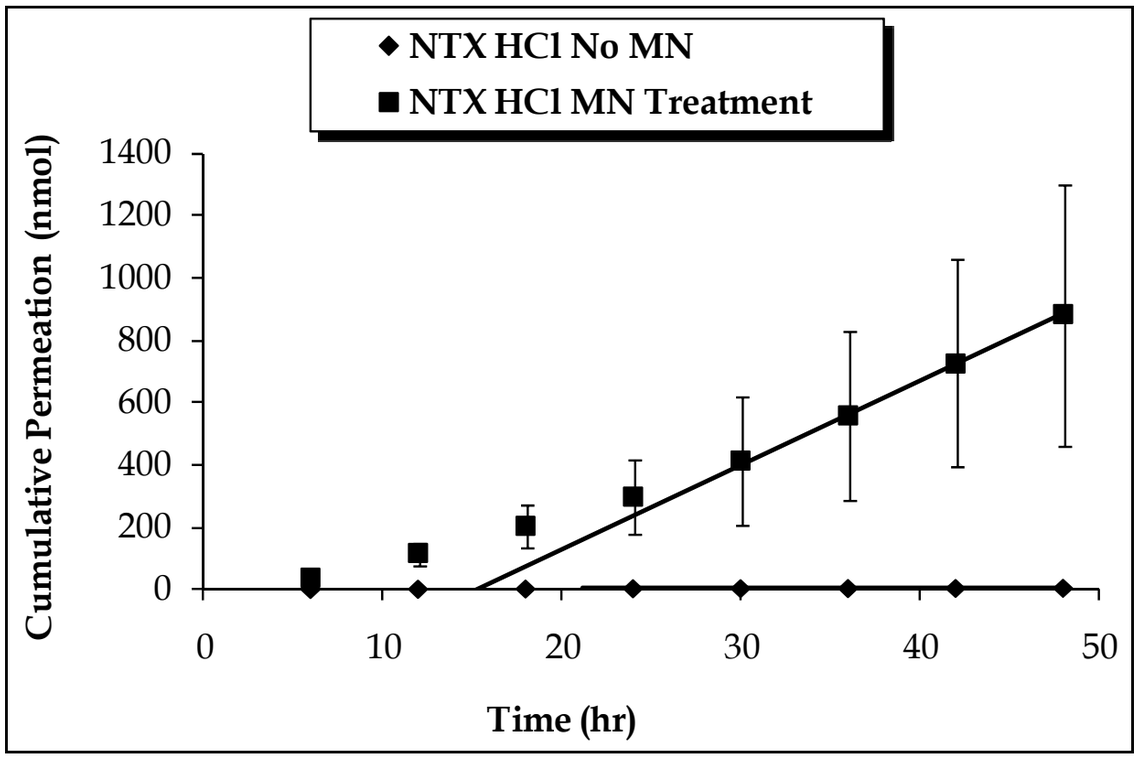

Fig. 3. Permeation profile of cumulative amount of NTX·HCl permeation through 100 MN treated and intact full thick human abdominal skin.

3.3 *In vivo* MN assisted transdermal studies

3.3.1 LC-MS Validation

In the current method, modification of the assay reported by Valiveti et al (Valiveti et al., 2004b) was validated to ensure proper sample analysis. Both NTX and NTXOL standards were first prepared in individual acetonitrile stock solutions. A standard curve of 0.5, 1, 2.5, 5, 7.5, 10, 15, and 25 ng/ml was generated after dilution of the stock solution for analysis of NTX and NTXOL containing 40 ng/ml naloxone as an internal standard. The retention times for NTX, NTXOL and naloxone were 4.3 ± 0.02 minutes, 3.1 ± 0.03 minutes, and 5.4 ± 0.2 minutes, respectively. The LOD and LOQ determined for NTX was 0.5 ng/ml in acetonitrile, however the LOQ was determined to be 1.0 ng/ml in plasma, as plasma interference made the blank plasma and 0.5 ng/ml plasma standards indistinguishable by LC-MS. The standard curve correlation coefficient for NTX in acetonitrile was 0.995 as compared to 0.979 for NTX extracted from plasma. However, both of these standard curves had values greater than $r^2 = 0.95$, the minimum value needed. The LOD and LOQ determined for NTXOL was 0.5 ng/ml in acetonitrile. The LOQ was determined to be 0.5 ng/ml as well in the plasma as plasma interference from the blank did not have an overlapping effect. The standard curve correlation coefficient for NTXOL in acetonitrile was 0.996, as compared to 0.987 for NTXOL extracted from plasma. The average extraction efficiency of NTX from plasma as compared to NTX in acetonitrile was 86.0 ± 6.8 %. Plasma standards (5 and 10 ng/ml) were placed in a -70°C freezer and allowed to freeze. The samples were then warmed to room temperature, and this freeze-thaw was repeated a total of three times over a 3 hour period. The samples were then extracted and analyzed. The three 5 ng/ml freeze-thaw standards had an average standard to internal standard ratio of 0.08 ± 0.002 with a %RSD of 2.7%. The average ratio of freeze-thaw samples was compared to the ratio of 0.08 ± 0.006 from 6 freshly extracted plasma standards (5 ng/ml) suggesting no degradation was occurring. The three 10 ng/ml freeze-thaw standards had an average standard to internal standard ratio of 0.13 ± 0.01 with a %RSD of 11.1 %. The average ratio of freeze-thaw samples was compared to the ratio of 0.14 ± 0.008 from 6 freshly extracted plasma standards (10 ng/ml) suggesting no degradation was occurring. Six replicate plasma samples of 5 and 10 ng/ml each were extracted as described above and injected in duplicate. The average ratio of standard to internal standard for the 5 ng/ml was 0.08 ± 0.006 with a %RSD of 7.8%. The reproducibility of extraction was in good confidence with a low %RSD. The 10 ng/ml ratio of NTX standard to internal standard was 0.14 ± 0.008 with an even lower %RSD of 5.6%. The average internal standard area for NTXOL throughout the day was 40,966 ± 3,462 with a %RSD of 8.5%.

3.3.2 *In vivo* hairless GP studies

GP pharmacokinetic data from 15 MN insertions from a section of 5 MNs (Figure 1) and one 6.7 cm^2 occlusive protective patch containing 0.5 g 16.0% NTX.HCL gel can be observed in table 2 and plasma profiles of NTX are shown in figure 4.

The plasma concentration rapidly reached a steady state level and maintained an average plasma level of about 2.6 ng/ml for 48 hours. Conversely, without the aid of MN insertions no detectable levels of NTX were observed after placement of one 6.7 cm^2 patch containing 16.0 % NTX·HCl gel.

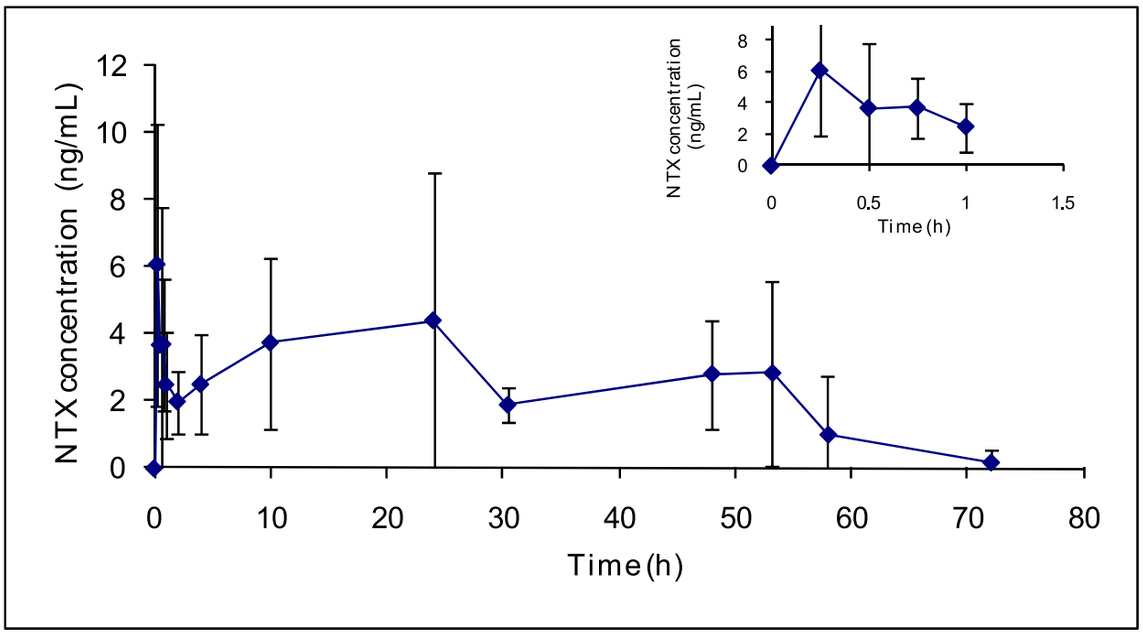

Fig. 4. Plasma NTX concentration profile from 16% NTX·HCl gel with 15 MN insertions in hairless GP.

	Healthy Human Subjects(*)		GP	
PK parameters	**NTX MN treatment**	**NTXOL MN treatment**	**NTX MN treatment**	**NTX No MN treatment**
C_{ss} (ng/ml)	**2.5 ± 1.0**	**0.6 ± 0.5**	**2.6 ± 0.6**	**ND**
T_{lag} (h)	**1.8± 1.1**	**1.4 ± 1.4**	**4.0 ± 0.0**	**ND**
AUC (ng/ml*h)	**142.9 ± 43.9**	**39.7 ± 25.9**	**158.2 ± 63.5**	**ND**
C_{max} (ng/ml)	**4.5 ± 2.4**	**1.9 ± 1.3**	**8.0 ± 1.8**	**ND**
T_{max} (h)	**8.8 ± 7.6**	**37.5 ± 31.3**	**0.3 ± 0.0**	**ND**
C_{last} (ng/ml)	**1.8 ± 1.0**	**0.4 ± 0.6**	**0.0 ± 0.0**	**ND**

(ND) NTX was not detected in the control (no MN) animals therefore PK parameters were not established.
(*) Human pharmacokinetic parameters are values obtained from earlier human study (Wermeling et al., 2008).

Table 2. Pharmacokinetic analysis of 6 healthy subjects and hairless GP treated with MN arrays and a 16.0% NTX·HCl gel patch.

3.3.3 *In vivo* human studies

We recently completed a human study with MN assisted transdermal delivery of NTX (Wermeling et al., 2008). Volunteers in the study wore four gel patch systems and were treated with a total of 400 MN insertions with an MN array as described by Wermeling et al.(Wermeling et al., 2008). Subjects reported no pain, only a sensation of pressure upon insertion of the MN arrays into each subjects upper arm region. As shown in table 2 the data exhibit a rapid increase in plasma NTX concentration above 2.5 ng/ml (therapeutic goal) within 2 hours and this level appears to remain for at least 48 hours. The average steady state concentration observed was 2.5 ± 1.0 ng/ml with 4 patches and a total of 100 MN insertions per patch (Wermeling et al., 2008).

3.3.4 *In vitro/In vivo* correlation

The average steady state plasma concentrations in GP and humans were estimated from equation 3 and were compared with the observed concentrations *in vivo* (Table 3). The average predicted steady state concentration in GP was 2.7 ± 0.7 ng/ml and the actual observed steady state concentration was 2.6 ± 0.6 ng/ml, using a clearance value of 5.65 L/h and a patch area of 6.7 cm^2 (Paudel et al., 2005). These two values were within 96% agreement with each other and there was no significant difference between the estimated and observed C_{ss} values ($p > 0.05$). Similarly, a good correlation was seen upon comparing human skin and healthy human individuals *in vivo*. The predicted and observed steady state concentrations in human skin and humans was 1.9 ± 0.7 ng/ml and 2.5 ± 1.0 ng/ml (Wermeling et al., 2008), respectively, using a clearance of 3.5 L/min and a patch area of 26.8 cm^2 (Vivitrol®).

Healthy Human Volunteers			**Hairless GP**	
(ng/ml)	**No MN**	**MN**	**No MN**	**MN**
C_{ss} Observed	**ND***	**2.5 ± 1.1***	**ND**	**2.6 ± 0.6**
C_{ss} Predicted	**0.01 ± 0.0**	**1.9 ± 0.7**	**0.5 ± 0.4**	**2.7 ± 0.7**
(nmol/cm^2/h)				
J_{ss} Observed	**0.13 ± 0.01**	**39.0 ± 13.1**	**1.1 ± 0.9**	**6.0 ± 1.5**
J_{ss} Predicted	**ND**	**51.9 ± 20.2**	**ND**	**5.8 ± 1.3**
% Correlation	**NC**	**76.0**	**NC**	**96.7**

(ND) No NTX detected in plasma
(NC) No correlation due to absence of NTX in plasma
(*) Results obtained from previous human study (Wermeling et al., 2008).

Table 3. *In vitro/in vivo* observed and predicted steady state fluxes and plasma concentrations of NTX in humans and hairless GP.

4. Discussion

4.1 *In vitro* diffusion studies

4.1.1 *In vitro* diffusion studies across full thickness hairless GP skin

Treatment of the GP skin with as little as 15 MN insertions caused an increase in flux and permeability compared to MN untreated skin. Permeability increased as the resistance from intact to MN treated skin decreased. Even with a minimal number of insertions, permeation was enhanced to a level that would be predicted to be observable in the hairless GP *in vivo*. Flux enhancement was 5.4 times higher with 15 MN insertions as compared to that of intact skin. Based on results from these experiments and previous other trials reported, the hairless GP model is a good choice for *in vitro* screening of transdermal candidates (Valiveti et al., 2004a; 2005).

4.1.2 *In vitro* diffusion studies across full thickness human skin

As observed with GP skin, an increase in both flux and permeability coefficient was observed in MN treated human skin compared to intact full thickness skin. Earlier work with 100 MN insertions in human skin gave a flux enhancement ratio of 8.3 in contrast to our 300 fold enhancement in flux and permeability coefficient (Banks et al., 2008). Differences between the formulations and concentration (10% vs. 16%), excess solid, and viscosity can definitely influence the NTX flux in the presence of MN micropores. A reduction in lag time when the skin is exposed to MNs is a strong indication that there has been a change in the diffusivity and/or permeation pathway. Thus, not only can flux indicate a change in the route of diffusion and resistance of the skin, but also the lag time is a good indicator of the drug re-routing.

It is well established that a 2.5 ng/ml NTX plasma concentration in humans provides approximately an 85% narcotic blockade of a 25 mg IV injection of heroin (Verebey et al., 1976). It was predicted that an area of 26.8 cm^2 would be required to obtain a therapeutic NTX plasma level, based on the flux information presented in table 1 and figure 3, and the gel formulation used. Thus, a four patch 16% NTX.HCl gel system with 100 MN insertions per patch was proposed to determine the feasibility of MN assisted delivery in humans (Wermeling et al., 2008).

4.2 *In vivo* MN assisted transdermal studies

4.2.1 *In vivo* hairless GP studies

Of importance in GP studies was a rapid increase in NTX plasma concentration to steady state and that C_{ss} remained reasonably constant for at least 48 hours after 15 MN treatment. Steady state concentrations remaining constant for 48 hours compares with earlier work, where NTXOL plasma concentrations, transepidermal water loss, and microscopic staining and visualization of pores over time were also consistent for 48 hours (Banks et al., 2010). No detectable levels of NTX were observed in GP without MN insertions. As expected, one would not likely see quantifiable amounts *in vivo* due to the lack of a significant amount of pore pathways, such as sweat glands or follicles, through which hydrophilic NTX could permeate. However, even with as little as 15 MN insertions to the skin a rapid increase in flux is observed and the MN created aqueous pores remain open. The steady-state profile of NTX concentrations in the plasma prior to 48 h when the pores begin to close suggests that

once treated with an MN array a constant flow is created for a substantial period. These micropores could theoretically create a more precise and controlled release of drug delivery, as compared to passive delivery systems that rely on inter-individual variations in stratum corneum lipid bilayer resistance. As well, the initial "burst" observed in the plasma concentrations could be caused from a rapid influx of the drug followed by the attainment of the equilibrium steady-state flow through the aqueous channels and constant permeation rates. The "burst" effect in the plasma concentration profile circumvents one of the major complaints about transdermal delivery, the typically long lag times. Drug therapies like transdermal fentanyl could benefit from a "burst" effect as a bolus dose, followed by maintenance therapy for at least 48 hours. Thus, the MN gel patch assembly appears to be a successful candidate for the transdermal delivery of NTX in the GP model.

4.2.2 *In vivo* human studies

As previously described, there are limited successful treatments for opiate and alcohol abuse with NTX (Vivitrol®; PDR, 1996). In a recent study, a therapeutic approach to MN transdermal delivery of NTX in healthy human volunteers was completed (Wermeling et al., 2008). As seen in the GP experiment, there was a rapid initial increase in the plasma drug concentration followed by controlled release of NTX in these human volunteers. For opiate and alcohol abusers, a fast acting form of NTX is desirable and achieving a steady-state permeation of NTX and maintaining that rate for an extended time will benefit addiction therapy. C_{max}, an important PK parameter, was rapidly achieved in all six subjects (4.5 ± 2.4 ng/ml), and this onset was observed within a relatively short time (8.8 ± 7.6 h) (Wermeling et al., 2008). No plasma levels were observed in human non-MN controls. NTXOL plasma levels were lower than NTX, but the same overall permeation profile shape was observed as compared to NTX. *In vivo* human data including C_{ss} and other PK parameters in table 2 had very little subject to subject variability (Wermeling et al., 2008). Conversely, after oral administration, there appears to be a much higher degree of variability in humans, as much as eight-fold (Meyer et al., 1984; Rukstalis et al., 2000). Not only did the study prove that a water soluble molecule could be delivered through an MN-created pore, but delivery rates were in a therapeutic range for a poorly bioavailable NTX (Wermeling et al., 2008).

4.2.3 *In vitro/in vivo* correlation

Using equation 3 to predict the steady state concentration *in vivo* or the steady state flux *in vitro*, a correlation can be made to determine the likeness of the *in vitro* model to actual *in vivo* pharmacokinetic evaluation of a compound. During this research both the *in vitro* and *in vivo* studies proved to be highly successful. There was no significant difference between the estimated and observed C_{ss} values in GP. The GP *in vitro* skin model, therefore, is an excellent *in vitro* based set up to screen potential candidates for MN enhanced transdermal delivery. Previous studies from our group has shown GP as a good model for NTX prodrugs and other highly lipophilic compounds for passive delivery (Valiveti et al., 2004a; 2005). However, this is the first time a study has shown good *in vitro* and *in vivo* correlation in GPs for MN assisted transdermal delivery. The percent correlation between human and human skin was 76%, which showed an under estimation for the *in vitro* studies. This could be due in fact to the location of the patches worn by volunteers compared to the area of skin used for *in vitro* studies. The patches were placed on the upper region of the arm as

compared to the full thickness abdominal skin used for *in vitro* permeation studies. Another reason may be the enzymatic activity differences in human skin *in vitro and in vivo*. It may also be possible that polar NTX also has significant diffusion through follicular routes in the skin *in vivo*. Overall, however, a good correlation between the *in vitro* and *in vivo* studies was observed in both GP skin and GP as well as in human skin and healthy human volunteers. Either skin type could be utilized with confidence when screening compounds for MN enhanced permeation studies *in vitro*.

5. Conclusion

In the present study, the aim was to evaluate the transdermal delivery efficiency of NTX·HCl salt via MN enhancement of skin in both *in vitro* and *in vivo* studies. In human and GP skin, excellent MN enhancement was observed as compared to intact skin. The same trend was observed *in vivo* and it was shown that a therapeutic plasma level could be achieved and maintained for at least 48h in human subjects, whereas no plasma levels were observed in either human or GP non-MN treated controls. Overall, an excellent IVIVC was observed between humans and human skin, as well as GP and GP skin. Thus, both human and GP *in vitro* models are excellent cost saving and predictive models for MN enhanced transdermal candidate screening. In regards to future applications, the work lies in developing a patch system that is patient friendly and cost effective for the treatment of alcoholism. Such work is ongoing in the lab of Dr. Audra Stinchcomb to develop a microneedle and patch system that can be effectively transitioned to the market for the treatment of alcohol abuse.

6. Acknowledgments

We would like to thank Dr. Mark Allen, Dr. Harvinder S. Gill and Dr. Mark R. Prausnitz at Georgia Tech for the use of microfabrication facilities and fabrication of microneedles. This research was supported in part by NIH R01DA13425. MRP is a member of the Center for Drug Design, Development and Delivery and the Institute for Bioengineering and Bioscience at Georgia Tech. MRP is the Emerson Lewis Faculty Fellow.

7. References

Banks, SL., Paudel, KS., Brogden, NK., Loftin, CD., & Stinchcomb, AL. (2011). Diclofenac enables prolonged delivery of naltrexone through microneedle-treated skin. *Pharm Res*, Vol.28, No.5, pp. 1211-11219, ISSN 1573-904X.

Banks, SL., Pinninti, RR., Gill, HS., Crooks, PA., Prausnitz, MR., & Stinchcomb, AL. (2008). Flux across of microneedle-treated skin is increased by increasing charge of naltrexone and naltrexol in vitro. *Pharm Res*, Vol.25, No.7, pp. 1677-1685, ISSN 0724-8741.

Banks, SL., Pinninti, RR., Gill, HS., Paudel, KS., Crooks, PA., Brogden, NK., Prausnitz, MR., & Stinchcomb, AL. (2010). Transdermal delivery of naltrexol and skin permeability

lifetime after microneedle treatment in hairless guinea pigs. *J Pharm Sci.* Vol.99, No.7, pp. 3072-3080, ISSN 1520-6017.

Cormier, M., Johnson, B., Ameri, M., Nyam, K., Libiran, L., Zhang, DD., & Daddona, P. (2004). Transdermal delivery of desmopressin using a coated microneedle array patch system. *J Control Release*, Vol.97, No. 3, pp. 503-511.

Coulman, SA., Barrow, D., Anstey, A., Gateley, C., Morrissey, A., Wilke, N., Allender, C., Brain, K., Birchall, JC. (2006). Minimally invasive cutaneous delivery of macromolecules and plasmid DNA via microneedles. *Curr Drug Deliv,* Vol.3, No 1, pp. 65-75., ISSN 1567-2018.

FDA. Guidance for industry, extended release oral dosage form: development, evaluation and application of an in vitro/in vivo correlation, 04.08.2011, Available from http://www.fda.gov/downloads/Drugs/GuidanceComplianceRegulatoryInformation/Guidances/ucm070239.pdf

Gardeniers, JGE., Luttge, JW., Berenschott, JW., de Boer, MJ., Yeshurun, Y., Hefetz, M., van't Oever, R., & van den Berg, A. (2003). Silicon micromachined hollow microneedles for transdermal liquid transport. *J MEMS*, Vol.6, pp. 855-862.

Hammell, DC., Hamad, M., Vaddi, HK., Crooks, PA., & Stinchcomb, AL. (2004). A duplex "Gemini" prodrug of naltrexone for transdermal delivery. *J Control Release*, Vol. 97, No. 2, pp. 283-290.

Hussain, MA., Koval, CA., Myers, MJ., Shami, EG., & Shefter, E. (1987). Improvement of the oral bioavailability of naltrexone in dogs: a prodrug approach. *J Pharm Sci,* Vol.76, No.5, pp. 356-358.

King, AC., Volpicelli, JR., Gunduz, M., O'Brien, CP., & Kreek, MJ. (1997). Naltrexone biotransformation and incidence of subjective side effects: a preliminary study. *Alcohol Clin Exp Res*, Vol.21, No.5, pp. 906-909, ISSN 0145-6008.

Kiptoo, PK., Hamad, MO., Crooks, PA., & Stinchcomb, AL. (2006). Enhancement of transdermal delivery of 6-beta-naltrexol via a codrug linked to hydroxybupropion. *J Control Release,* Vol.113, No.2, pp. 137-145, ISSN 0168-3659.

Martanto, W., Davis, SP., Holiday, NR., Wang, J., Gill, HS., & Prausnitz, MR. (2004). Transdermal delivery of insulin using microneedles in vivo. *Pharm Res,* Vol.21, No.6, pp. 947-952.

Meyer, MC., Straughn, AB., Lo, MW., Schary, WL., & Whitney, CC. (1984). Bioequivalence, dose-proportionality, and pharmacokinetics of naltrexone after oral administration. *J Clin Psychiatry*, Vol.45, No. 9 Pt 2, pp. 15-19.

Milewski, M., & Stinchcomb, AL. (2011). Vehicle composition influence on the microneedle-enhanced transdermal flux of naltrexone hydrochloride. *Pharm Res,* Vol.28, No.1, pp. 124-134, ISSN 1573-904X.

Milewski, M., Yerramreddy, TR., Ghosh, P., Crooks, PA., & Stinchcomb, AL. (2010). In vitro permeation of a pegylated naltrexone prodrug across microneedle-treated skin. *J Control Release,* Vol.146, No.1, pp. 37-44, ISSN 1873-4995.

Mikszta, JA., Alarcon, JB., Brittingham, JM., Sutter, DE., Pettis, RJ., & Harvey, NG. (2002). Improved genetic immunization via micromechanical disruption of skin-barrier function and targeted epidermal delivery. *Nat Med*, Vol.8, No.4, pp. 415-419, ISSN 1078-8956.

Paudel, KS., Nalluri, BN., Hammell, DC., Valiveti, S., Kiptoo, P., Hamad, MO., Crooks, PA., & Stinchcomb, AL. (2005). Transdermal delivery of naltrexone and its active metabolite 6-beta-naltrexol in human skin in vitro and guinea pigs in vivo. *J Pharm Sci*, Vol.94, No.9, pp. 1965-1975.

PDR. (1996). Generics second edition. Medical Economics. New Jersey, pp. 1083-1086

Pillai, O., Nair, V., & Panchagnula, R. (2004). Transdermal iontophoresis of insulin: IV. Influence of chemical enhancers. *International Journal of Pharmaceutics*, Vol.269, No.1, pp. 109-120.

Prausnitz, MR. (2004). Microneedles for transdermal drug delivery. *Adv Drug Deliv Rev*, Vol.56, No.5, pp. 581-587.

Prausnitz, MR., Mikszta, JA., & Raeder-Devens, J. (2005). Microneedles, In: *Percutaneous Penetration Enhancers*, (Ed. EW Smith and HI Maibach), 239-255, CRC Press, Boca Raton, FL.

Rukstalis, MR., Stromberg, MF., O'Brien, CP., & Volpicelli, JR. (2000). 6-beta-naltrexol reduces alcohol consumption in rats. *Alcohol Clin Exp Res*, Vol.24, No.10, pp. 1593-1596.

Vaddi, HK., Hamad, MO., Chen, J., Banks, SL., Crooks, PA., & Stinchcomb, AL. (2005). Human skin permeation of branched-chain 3-0-alkyl ester and carbonate prodrugs of naltrexone. *Pharm Res,* Vol.22, No.5, pp. 758-765.

Valiveti, S., Paudel, KS., Hammell, DC., Hamad, MO., Chen, J., Crooks, PA., & Stinchcomb, AL. (2005). In vitro/in vivo correlation of transdermal naltrexone prodrugs in hairless guinea pigs. *Pharm Res,* Vol.22, No.6, pp. 981-989.

Valiveti, S., Hammell, DC., Earles, DC., & Stinchcomb, AL. (2004a). In vitro/in vivo correlation studies for transdermal delta 8-THC development. *J Pharm Sci,* Vol. 93, No.5, pp. 1154-1164.

Valiveti, S., Nalluri, BN., Hammell, DC., Paudel, KS., & Stinchcomb, AL. (2004b). Development and validation of a liquid chromatography-mass spectrometry method for the quantitation of naltrexone and 6 beta-naltrexol in guinea pig plasma. *J Chromatogr B Analyt Technol Biomed Life Sci,* Vol.810, No.2, pp. 259-267.

Verebey, K., Volavka, J., Mule, SJ., & Resnick, RB. (1976). Naltrexone: disposition, metabolism, and effects after acute and chronic dosing. *Clin Pharmacol Ther,* Vol.20, No.3, pp. 315-328.

Vivitrol™ (naltrexone for extended-release injectable suspension, 04.08.201, Available from http://www.vivitrol.com/

Volpicelli, JR., Alterman, AI., Hayashida, M., O'Brien, CP. (1992). Naltrexone in the treatment of alcohol dependence. *Arch Gen Psychiatry*, Vol.49, No.11, pp. 876-880.

Wermeling, DP., Banks, SL., Hudson, DA., Gill, HS., Gupta, J., Prausnitz, MR., & Stinchcomb, AL. (2008). Microneedles permit transdermal delivery of a skin-impermeant medication to humans. *Proc Natl Acad Sci USA*. Vol.105, No.6, pp. 2058-2063, ISSN 1091-6490.

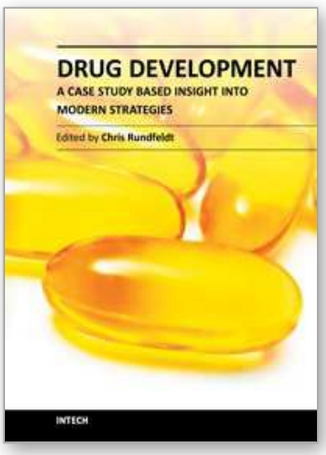

Drug Development - A Case Study Based Insight into Modern Strategies

Edited by Dr. Chris Rundfeldt

ISBN 978-953-307-257-9
Hard cover, 654 pages
Publisher InTech
Published online 07, December, 2011
Published in print edition December, 2011

This book represents a case study based overview of many different aspects of drug development, ranging from target identification and characterization to chemical optimization for efficacy and safety, as well as bioproduction of natural products utilizing for example lichen. In the last section, special aspects of the formal drug development process are discussed. Since drug development is a highly complex multidisciplinary process, case studies are an excellent tool to obtain insight in this field. While each chapter gives specific insight and may be read as an independent source of information, the whole book represents a unique collection of different facets giving insight in the complexity of drug development.

How to reference

In order to correctly reference this scholarly work, feel free to copy and paste the following:

Stan L. Banks, Audra L. Stinchcomb and Kalpana S. Paudel (2011). Microneedle-Assisted Transdermal Delivery of Opioid Antagonists for the Treatment of Alcoholism, Drug Development - A Case Study Based Insight into Modern Strategies, Dr. Chris Rundfeldt (Ed.), ISBN: 978-953-307-257-9, InTech, Available from: http://www.intechopen.com/books/drug-development-a-case-study-based-insight-into-modern-strategies/microneedle-assisted-transdermal-delivery-of-opioid-antagonists-for-the-treatment-of-alcoholism

INTECH
open science | open minds

InTech Europe
University Campus STeP Ri
Slavka Krautzeka 83/A
51000 Rijeka, Croatia
Phone: +385 (51) 770 447
Fax: +385 (51) 686 166
www.intechopen.com

InTech China
Unit 405, Office Block, Hotel Equatorial Shanghai
No.65, Yan An Road (West), Shanghai, 200040, China
中国上海市延安西路65号上海国际贵都大饭店办公楼405单元
Phone: +86-21-62489820
Fax: +86-21-62489821

IntechOpen